Structural and Optical Study of SnO Nanoparticles Synthesized Using Microwave–Assisted Hydrothermal Route

P. Boroojerdian

Department of Passive Defense, Malek Ashtar University of Technology, Tehran, I. R. Iran

(*) Corresponding author: boroojerdian89@gmail.com

Abstract:

SnO nanoparticles were synthesized using microwave–assisted hydrothermal method. It was noticed that at 300 and 600 watt microwave power, SnO formed and remained in the tetragonal phase. At 900 watt, SnO_2 started appearing and a mixture of SnO and SnO_2 phases coexisted. The particle size varied from ~2 to ~13 nm at 300 to 900 watt radiation power. The UV-V absorption spectra showed the excitonic peaks of ~288, ~300 and ~315 nm corresponding to crystal sizes of ~2, ~6 and ~10 nm, respectively. For particles larger than 10 nm, no excitonic peak was observed. The appearance of these excitonic peaks could be attributed to the conversion of indirect band gap in bulk SnO to direct band gap in SnO nanoparticles. To verify this assumption, photoluminescence spectroscopy was carried out. The results showed a strong emission of 677 nm upon excitation at 336 nm wavelength, confirmed the assumption.

Keywords: SnO, Nanoparticles, Microwave–Assisted Synthesis, Semiconducting Material.

1. INTRODUCTION

Over the last few decades, it was well established [1-3] that below a particular size, physico–chemical properties of semiconducting materials become size dependent. This phenomenon attracted wide attention to the integration of optically and electrically active semiconducting materials after nanostructured silicon was observed to show strong photoluminescence [4,5], although bulk Si is an indirect band gap semiconducting material and hence non-radiative. This feature could allow the synthesis of more optically as well as electrically active materials.

SnO, which is a wide indirect band gap semiconducting material, has recently attracted attention because of its various applications. SnO can be suitably used in rechargeable lithium batteries [6,7], as a coating material, as a catalyst for cyclization of maleamic acid, for the polymerization of lactic acid [8-11], as a precursor of SnO_2 [12,13] which is widely used in transparent oxide semiconductor electrodes [14] and gas sensors [15,16].

A variety of techniques such as wet chemical [17,18], sonochemical [19] and microwave–assisted hydrothermal routes [20,21] were employed to achieve nanoparticles of SnO. Among these, the microwave-assisted hydrothermal method of synthesizing SnO attracted more attention for its simplicity, purity, short time of synthesis and better control of crystal size; the ultrahigh frequency (GHz) of microwaves creates tremendous intermolecular movement and friction, which causes thermal and non-thermal effects [22]. SnO is metastable at

Table 1: *Concentration, conditions and positions of exitonic peaks of hydrothermal treatment applied to the starting solutions*

Sample	Base molarity	Microwave power (w)	Time (minute)	Excitonic peak (nm)
SnO-300-20	0.01	300	20	288
SnO-300-30	0.01	300	30	291
SnO-300-40	0.01	300	40	293
SnO-300-50	0.01	300	50	295
SnO-600-20	0.01	600	20	300
SnO-600-30	0.01	600	30	302
SnO-600-40	0.01	600	40	305
SnO-600-50	0.01	600	50	307
SnO-900-20	0.01	900	20	315
SnO-900-30	0.01	900	30	317
SnO-900-40	0.01	900	40	318
SnO-900-50	0.01	900	50	321

normal conditions and often SnO and SnO_2 coexist either due to oxidation of SnO or reduction of SnO_2 [23]. However, Pires and coworkers [24] only reported the synthesis of SnO powders with sizes ranging from 30nm to 2 µm, and so no excitonic peak was observed as their size exceeded the Bohr radius.

Below, a single phase synthesis of pure SnO nanoparticles in aqueous solution obtained by the microwave heating at 100ºC was reported.

2. PROCEDURE

A 100ml aqueous solution (0.01M and pH=1.4) was prepared by dissolving appropriate amount of $SnCl_2.2H_2O$ in dilute HCl. The solution was continuously stirred while ethylenediamine ($H_2NCH_2 CH_2NH_2$) was added drop by drop to obtain a precipitate, and pH of the solution was increased to 5. The precipitate was washed several times to remove excess ions, which was then dispersed in water, and exposed to microwave radiation (Samsung, Combi model 2.4 GHz). A number of samples were prepared to investigate the effect of different powers and durations of microwave radiation. The radiation power was changed ranging from 300 to 900 watt and the irradiation timing from 20 to 50 minutes.

The sample characteristics were displayed by using techniques such as X-Ray diffraction (XRD-Philips, PW1830), UV-Vis spectrophotometry (HitachiUV-Vis3310), photoluminescence spectrophotometry (Perkin Elmer, LS-55) transmission electron microscopy (TEM Philips, EM 2085, 120KeV) and scanning tunneling microscopy (STM, Natsyco - ss/l).

3. RESULTS AND DISCUSSION

Figure1 illustrates the X-ray diffraction patterns of SnO samples prepared under different microwave powers (300 to 900 W) for 20 minute duration. The diffraction pattern of the sample irradiated at 300

W shows several broad peaks that are attributed to the tetragonal phase of SnO (JCPDSS-85-423) [25]. However, the sample treated at 600 W (showing only SnO phase) has more intense peaks and smaller FWHM, which is an indication of the particle growth. The XRD patterns also have a resemblance to the diffraction patterns shown in ref [19, 22, 25].
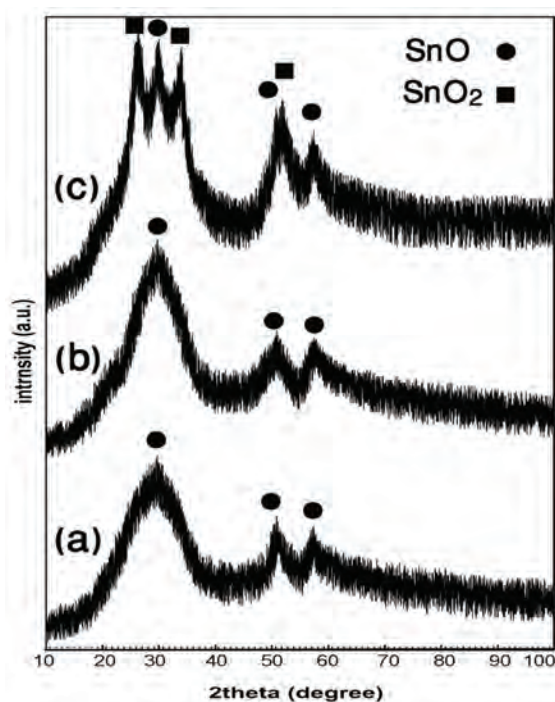

Figure 1: *XRD patterns of the SnO nanoparticles prepared under different microwave power a) 300 W, b) 600 W and c) 900 W*

The diffraction pattern for the sample treated at 900 W is complex since an additional SnO_2 phase also appears (JCPDS-88-0287) [25]. It seems that at higher radiation power, SnO partially oxidized to form SnO_2. By comparing the level of the intense peaks of SnO and SnO_2 in the XRD patterns, it can be deduced that SnO forms only 46 % of the sample, and SnO_2 is dominating. Mean particle sizes are determined by using Scherrer's formula and considering the highest peaks at (2θ=29.875 °)

$$d = \frac{0.9\lambda}{B\cos\theta} \tag{1}$$

Where λ is wavelength of X-ray radiation

($Cu_{k\alpha}$=1.5418 Å) and B is full width at half maxima of the peak. The calculated size (from Figure1), varies from ~3 nm for 300 W, to ~7 nm for 600W radiation power. At 900 W it increases to a value of ~10.4 nm.

Optical absorption spectra of various SnO samples are shown in Figure2. The reported band gap value of SnO is 2.5-3eV and the absorption peak is at 413-496 nm as expected, with no excitonic peak (no quantum size effect). An excitonic peak is evident at~288nm (~4.30eV) for the sample irradiated at 300 watt for 20 minutes. The absorption spectra seen in figures 2a,b is only the quantum size effect of SnO phase (from Figure 1a,b) and figure 2c is that of the mixed phases.

Figure 2d shows the absorption spectrum of ~2 nm pure SnO_2 sample, synthesized under identical condition and the inset shows the XRD pattern of the same. The excitonic peak situated at ~260 nm is obviously different from that of the pure SnO sample. The red arrows in Figure 2c point to two weak humps in the absorption spectra of the samples irradiated for 20 and 40 minutes. Considering the excitonic peak in the absorption spectrum of pure SnO_2 nanoparticles (Figure 2d) these humps can be attributed to the presence of the SnO_2 nanoparticles in the samples irradiated at 900 W power. The result is in good agreement with the XRD pattern of the sample. For the samples treated at 600 and 900 W for 20 minutes (Figure2b,2c), the excitonic peaks shifted to ~300 nm (~4.13 eV) and ~315 nm (~3.93 eV), respectively. For the sample with crystal size larger than ~10 nm (bulk-like), no excitonic peak is observed. It can be seen that, the excitonic peaks for the samples have shifted from ~315 nm to ~288 nm corresponding to energy gaps from ~3.93 eV to ~4.30 eV, respectively. Here, by using microwave radiation in a polar solvent (i.e. water), very high and uniform heating is provided which in turn provides a uniform environment for nucleation [26]. This might be a reason that microwave–assisted hydrothermal route improves the reaction.

In table 1, the positions of excitonic peaks (energy gap) for the samples irradiated for various durations and power are given. It can be seen that, when shorter duration and lower powers of microwave
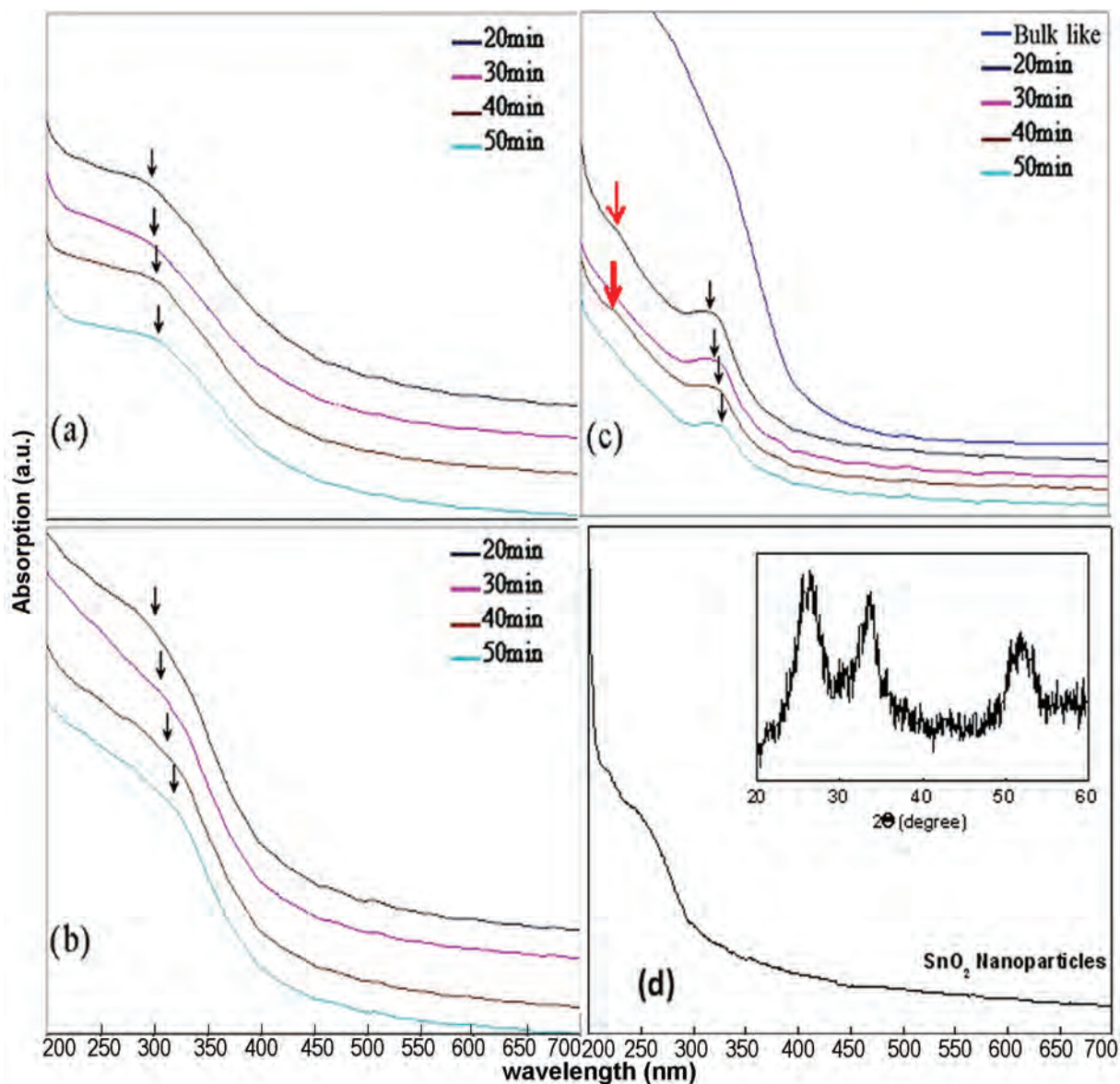
Figure 2: Optical absorption spectra of SnO nanoparticles prepared under different microwave power a) 300 W, b) 600 W and c) 900 W for various timing. d) Optical absorption of SnO$_2$ nanoparticles with the respective XRD pattern (inset).

are used, smaller crystals with excitonic peaks at shorter wavelengths were obtained. Between 20 and 50 minute irradiation, the crystals grow and the excitonic peaks appear at longer wavelengths. Here the characteristics of absorption spectra are similar to those reported in direct band gap semiconductor nanoparticles of CdS and ZnS [27, 28]. The versatile technique for confirming radiative nature of semiconducting materials is photoluminescence

spectroscopy. Figure3 illustrates excitation and emission spectra of SnO sample. The excitation spectrum shows one strong band at 336 nm and two weak bands centered at ~295 and 390 nm, consistent with the results of the absorption spectra. The emission spectrum shows one narrow strong band at 677 nm which is obviously different from the reported values for the SnO$_2$ nanoparticles (i.e. $\lambda_{excitation}$ = 300 nm and $\lambda_{emission}$ = 400 nm) [29].
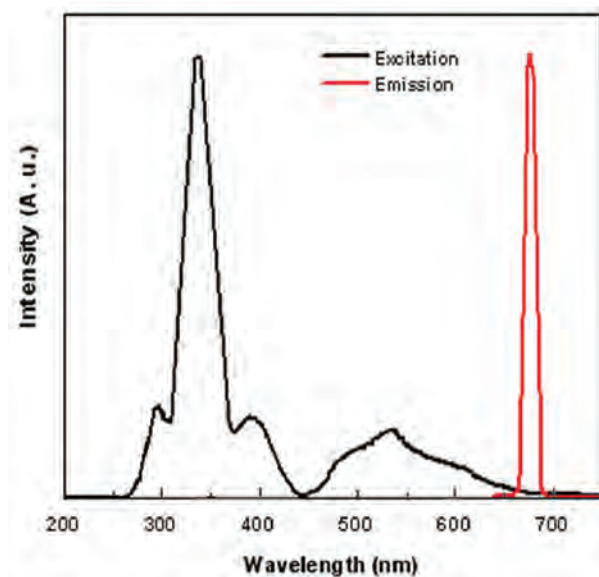
Boroojerdian

Figure 3: *Photoluminescence spectrum of SnO nanoparticles.*

Therefore, because of quantum confinement, the indirect band gap of bulk SnO is converted to a direct band gap. Similar behavior has been reported in other indirect band gap semiconductors like Si and Ge [5, 30].

In order to confirm the size and shape of the crystals, STM and TEM micrographs were taken for the samples irradiated at various powers for 20 minutes. Figure4 with insets showing the corresponding particle size histograms, indicates that the particles are spherical and relatively monodispersed with sizes varying between ~2 and 13 nm.

4. CONCLUSIONS

By using microwave radiation, monodispersed SnO nanoparticles of various sizes have been obtained. Depending on the radiation power and duration, the SnO nanoparticles obtained were completely pure or contained some SnO_2 in some samples. The SnO samples show strong excitonic peaks in the UV-V absorbance spectra which is absent in bulk SnO. Blue shift in the position of the excitonic
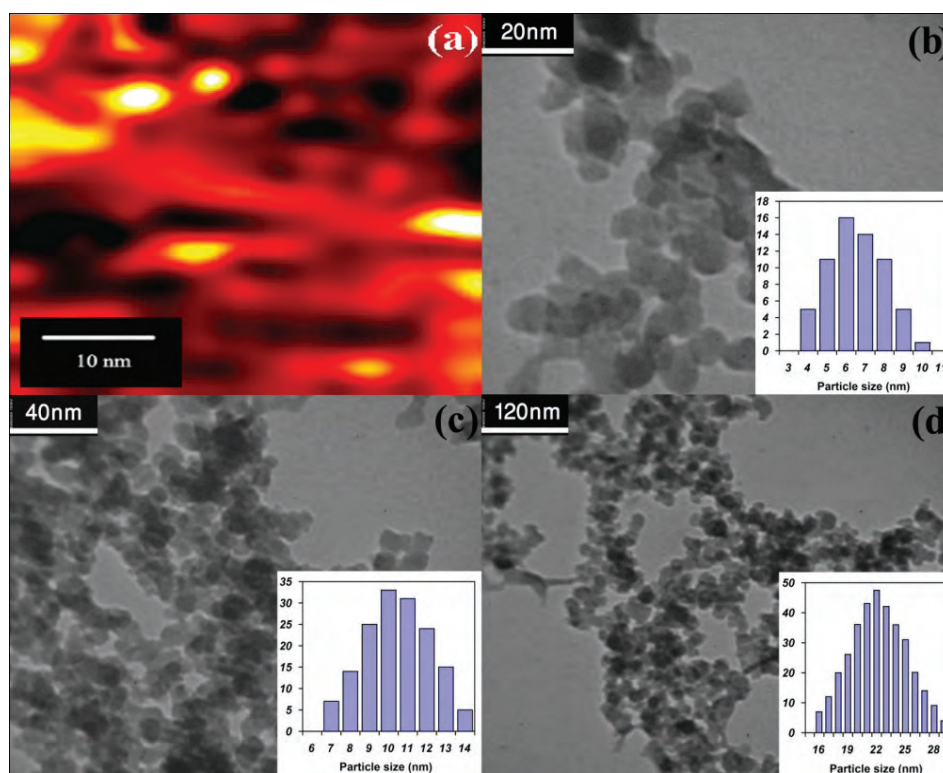

Figure 4: *a) STM micrograph of the sample treated at 300 W and TEM images of the SnO powders treated at b) 600 W c) 900 W all for 20 minutes and d) bulk-like sample.*

peak to ~288 nm corresponding to an energy gap of 4.30 eV was observed for the smallest particle size. The sample also showed very strong peak in the photoluminescence emission spectrum indicating that SnO nanoparticles have become highly radiative. Therefore, it can be concluded that SnO nanoparticles have become a direct band gap semiconducting material. Monodispersity, morphology and size of the particles were realized from STM and TEM images.

REFERENCES

1. Y. Nosaka, K.Yamaguchi, H. Miyama, M. Hayashi: Chem. Lett. Vol. 16, (1988), pp. 605-608.

2. A.R.Kortan, R. Hull, R.L.Oplia, M.G.Banwendi, M.L.steiggerwald, P.L.Carrol: J. Am.Chem. Soc., Vol. 12, (1990), pp. 1327-1332.

3. N.Herron, Y.Wang, H.Eckert: J. Am. Chem. Soc., Vol. 12, (1990), pp. 1322-1326.

4. L. T. Canham: Appl. Phys. Lett. Vol. 57, (1990), pp. 1046-1050.

5. C. Harris, E. P. O'Reily: Physica E, Vol. 32, (2006), pp. 341-345.

6. Y. Idota, A. Matsufuji, Y. Mackawa, T. Miyasaka: Mater. Sci., Vol. 276, (1997), pp.1395-1397.

7. I. A.Courtney, J.R. Dahn: J. Electrochem Soc., Vol. 144, (1997), pp. 2045-2052.

8. Z. Han, N.Guo, F. Li, W. Zhang, H. Zhao, Y. Quian: Mater. Lett., Vol. 48, (2001), pp. 99-103 (and ref. there in).

9. W. Liu, X. Huang, Z. Wang, H. Li, L. Chen: J. Electrochem. Soc., Vol. 145, (1998), pp. 49-52.

10. O. Mao, R.L. Turner, I.A. Courtney, B.D. Fredericksen, M.I. Buckett, L.J. Krause: Electrochem. Solid-State Lett., Vol. 2, (1999), pp. 3-5.

11. N. Li, C. Martin: J. Electrochem. Soc., Vol. 148, (2001), pp. A164-170.

12. Z. R. Dai, Z.W. Pan, Z.L. Wang: J. Am. Chem. Soc., Vol. 124 ,(2002), pp. 8673-8680.

13. S. Wang, S.H. Xie, H.X. Li, S.R. Yan, K.N. Fan, M.H. Qiao: Chem. Commun., Vol. 12, (2005), pp. 507-509.

14. R.F. Presley, C.L. Munsee, C.H. Park, D. Hong, J.F. Wager, D.A. Keszler: J. Phys. D Appl. Phys., Vol. 37, (2004), pp. 2810-2813.

15. S.G. Ansari, S.K. Kulkarni, R.N. Karekar, R.C.Aiyer:J. Mat. Sci.Mater. Electr., Vol. 7, (1996), pp. 267-270.

16. S.G. Ansari, P. Boroojerdian,S.R. Sainkar, R.C. Aiyer, S.K. Kulkarni: Thin Solid Films, Vol. 295, (1997), 271-276.

17. Z.J. Jia, L.P. Zhu, G.H. Liao, Y. Yu, Y.W. Tang: Solid-State Commun., Vol. 132, (2004), pp. 79-82.

18. H. Deng, F.J. Lamelas, J.M. Hossenlopp: Chem. Mater., Vol. 15, (2003), pp. 2429-2436.

19. S. Majumdar, S. Chakraborty, P.S. Devi, A. Sen: Mater. Lett., Vol. 62, (2008), pp.1249-1251.

20. D.S. Wu, C.Y. Han, S.Y. Wang, N.L. Wu, I.A. Rusakova: Mater. Lett., Vol. 53, (2002), pp. 155-159.

21. T. Krishnakumar, N. Pinna, K.P. Kumari, K. Perumal, R. Jayaprakash: Mater. Lett., Vol. 62, (2008), pp. 3437-3440.

22. A.G. Saskia: Chem. Soc. Rev. Vol. 26, (1997), pp. 233-240.

23. H. Giefers, F. Porsch, G. Wortmann: Solid State Ionics, Vol. 176, (2005), pp. 199-207.

24. F.I. Pires, E. Joanni, R. Savu, M.A. Zaghete, E. Longo, J.A. Verela: Mater. Lett., Vol. 62, (2008), pp. 239-242.

25. Joint Committee on Powder Diffraction Standards, International Centre for Diffraction Data, Pennsylvania. (1991)

26. S.Tsunekawa., T.Fukuda., A. J. Kasuya: Appl. Phys., Vol. 87, (2000), pp. 1318-1321.

27. A.A. Khosravi, M. Kundu, G.S. Shekhawat, R.P. Gupta, A.K. Sharma, P.D. Vyas: Appl. Phys. Lett., Vol. 67, (1995), pp. 2506-2508.

28. M. Kundu, A.A. Khosravi, S.K. Kulkarni, P. Singh: J. Mater. Sci., Vol. 32, (1997), pp. 245-258.

29. F. Gu, S.F. Wang, C.F. Song, M.K. Lu, Y.X. Qi, G.J. Zhou, X. UD, D.R. Yuan: Chemical Physics Letters, Vol. 372, (2003), pp. 451-54.

30. A.N. Kholod, V.E. Borisenko, A. Saul, F.A. Avitaya, J. Fuhr: Optical Materials, Vol. 17, (2001), pp. 61-63.